Influence of Surface Charges on Impulse Flashover Characteristics of Alumina Dielectrics in Vacuum

Katsumi Kato, Hidenori Kato, Tsugunari Ishida, Hitoshi Okubo
Department of Electrical Engineering and Computer Science
Nagoya University
Furo-cho, Chikusa-ku, Nagoya, Aichi, 464-8603, Japan

and **Kenji Tsuchiya**
Hitachi, Ltd.
1-1, Kokubu-cho, 1-chome, Hitachi, Ibaraki, 316-8501, Japan

ABSTRACT

For higher electrical insulator performance of vacuum circuit breakers (VCB), the surface flashover in vacuum should be improved. In particular, it is important to clarify how strongly surface charges influence the surface flashover mechanism. In this paper, we investigated the surface flashover characteristics based on the existence of surface charges on an alumina insulator in vacuum. We changed the location and magnitude of surface charges and measured surface flashover voltage. From our experimental results, an attempt was made to clarify the influence of charges on alumina dielectrics on impulse surface flashover characteristics in vacuum. From this, we concluded that (1) when surface charges were located near the cathode electrode, a positive charge made the surface flashover voltage lower and a negative charge made the surface flashover voltage higher; and, (2) when surface charges were located in the way of the discharge path, both positive and negative charges made the surface flashover voltage lower. We were able to explain these results by considering the influence of surface charges on the electric field at flashover and on the secondary electron emission avalanche.

Index Terms = **Vacuum, surface flashover, surface charge, alumina insulator, electric field, secondary electron emission avalanche.**

1 INTRODUCTION

IN recent years, electrical insulation techniques in vacuum have become more important, because the vacuum circuit breakers (VCB) and vacuum interrupters (VI) applied up to medium voltage level are extending their application into higher voltage electric power systems. In order to enhance the operational voltage of VCB/VI, a high voltage electrical insulation technique in vacuum should be established [1].

From a practical point of view, the surface flashover characteristics of a solid insulator could be crucial in relation to the electric field concentration and surface charging [2, 3]. The electron emission from cathode triple-junction occurs and accumulates on the insulator surface. The accumulated charges distort the electric field distribution and could reduce the dielectric strength. In particular, the secondary electron emission avalanche (SEEA) phenomenon could be influenced strongly by the accumulated charge [4].

Although it is said that the SEEA can trigger off the surface flashover, the fundamental processes from SEEA to surface flashover have not yet been clarified. Because they are influenced by many factors of insulators, such as: the material properties, surface conditions, and surface charge distribution [4-7]. Therefore, it is important to clarify how strongly surface charges influence the surface flashover characteristics in vacuum.

Taking into consideration the aforementioned, we have been investigating the charging characteristics on an alumina surface in vacuum [8, 9]. The result revealed that surface charges were influenced by surface roughness and electric field distribution.

In this paper, we measured and investigated the dependence of the location and magnitude of surface charges on surface flashover characteristics.

2 EXPERIMENTAL SETUP

Figure 1 shows the experimental setup. Experiments were carried out in a 2.0×10^{-4} Pa vacuum. There were four motion feedthroughs for the experiments. In the vacuum chamber, we could generate the surface charge on the alumina surface and measure the 2-dimensional distribution of the surface potential with a surface potential meter.

Manuscript received on 25 November 2008, in final form 10 May 2009.

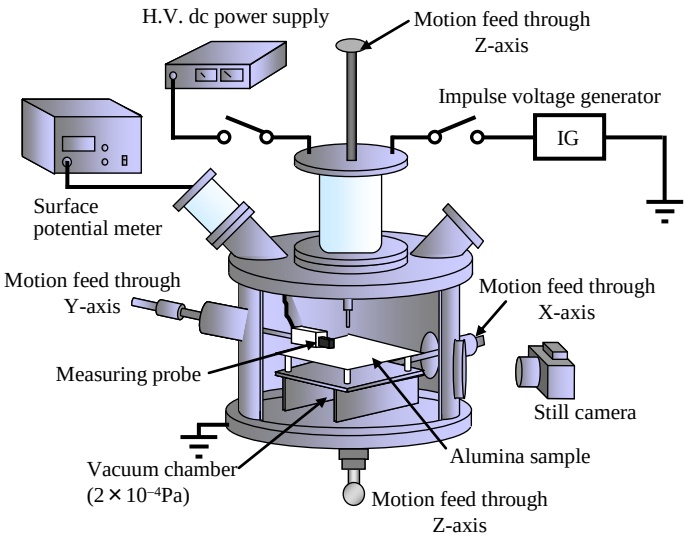

Figure 1. Experimental setup.

2.1 SURFACE CHARGE GENERATION

Figure 2 shows the electrode configuration for surface charge generation. We set up the high voltage rod electrode and alumina dielectrics (HA-92). The diameter of the rod electrode is 1 mm. The size of the alumina dielectric is 150 mm x 150 mm x 5 mm^t. We changed the vacuum gap length between the alumina plate and high voltage electrode by changing the position of the alumina plate. We measured the average surface roughness *Ra* with a film thickness meter (resolution 0.1 - 2.5 nm). The principle of the measurement is that the surface roughness is measured by the contact of the needle probe on the surface. Here, the deviation of the probe position is measured. The *Ra* of the alumina is 0.69 μm. We made a vacuum gap of 70 mm between the alumina dielectrics and ground electrode and arranged a background electrode 10 mm in width behind the alumina dielectrics to control the charging distribution.

In order to generate the surface charges on alumina dielectrics, we applied positive or negative dc ramped voltage (±0.1 kV/s, -25 kV to -35 kV or +25 kV to +35 kV) on the high voltage electrode. After that, the grounded electrode was placed under the alumina dielectrics, and we measured the 2-dimensional distribution of surface charging potential on alumina dielectrics with a surface potential meter. The measurement principle of the surface potential meter is a no contact vibrating capacitor with a measurement range of 0 to ±20 kV. In order to avoid the change of surface potential distribution by approaching the surface potential probe, the probe is automatically forced to apply the same potential to be measured.

The result of surface potential distribution is shown in Figure 3 as an example. Figures 3a and 3b show the negative and positive charge distributions, respectively. We found that the areas of surface charge were restricted to the width at the back electrode. In addition, by moving alumina dielectrics, the charging areas have changed their positions to A-D as shown in Figure 4.

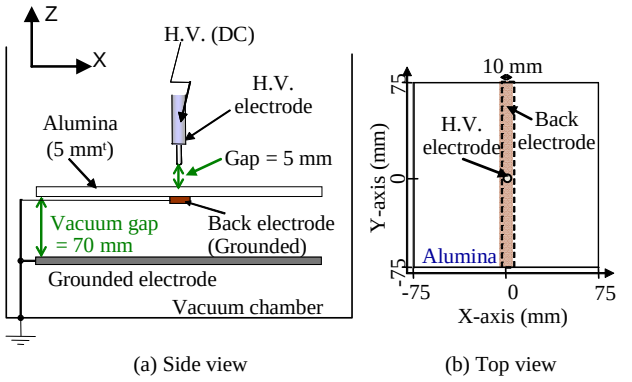

(a) Side view (b) Top view

Figure 2. Electrode configuration for surface charge generation.

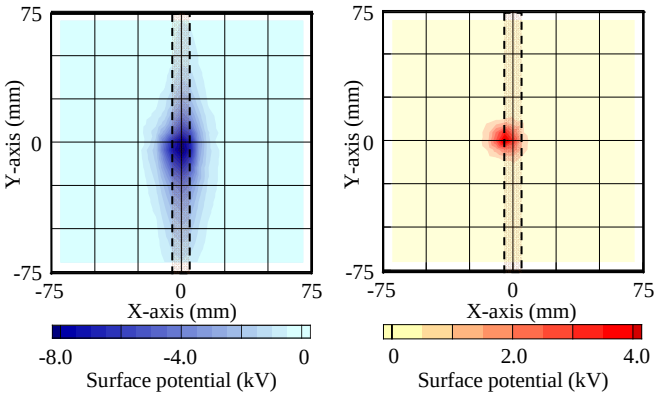

(a) Negative charge (applied voltage = -35 kV)

(b) Positive charge (applied voltage = +35 kV)

Figure 3. Positive and negative 2-D surface potential distribution.

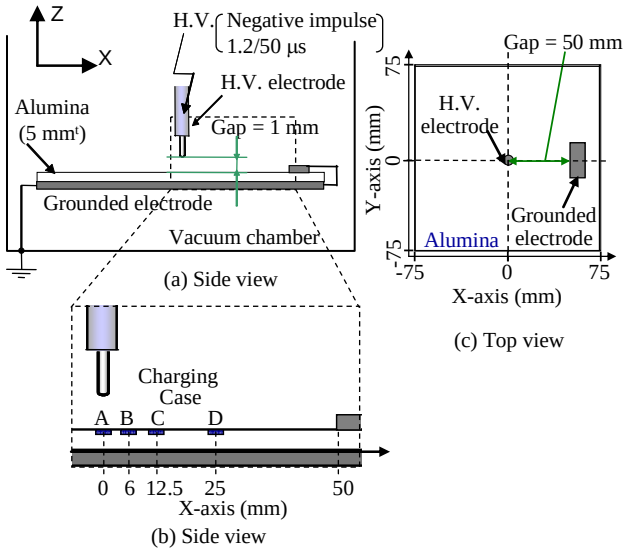

(a) Side view

(c) Top view

(b) Side view

Figure 4. Electrode configuration for surface flashover generation.

2.2 SURFACE FLASHOVER GENERATION

Figure 4 shows the electrode configuration for surface flashover generation. We made a vacuum gap of 1 mm between the alumina dielectrics and high voltage electrode, and arranged a grounded electrode at 50 mm distance from the high voltage electrode and back electrode under the alumina.

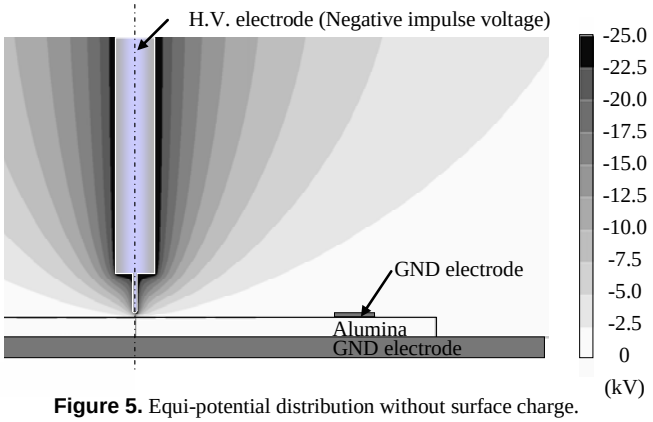

Figure 5. Equi-potential distribution without surface charge. (Applied voltage *Va* = -25 kV)

In order to generate surface flashover, we applied a negative impulse voltage (1.2/50 μs) to the high voltage electrode. We measured the potential surface distribution every time after we applied a negative impulse voltage to the high voltage electrode whether surface flashover was generated or not.

We measured the surface flashover voltage on alumina dielectrics. We changed charge magnitude and the location on the insulator below the high voltage electrode (Case A) and at the point that was 6, 12.5 and 25 mm distance from the high voltage electrode (Case B, C, D).

Figure 5 shows the calculation results of the equi-potential distribution without surface charges. We used the commercially available three-dimensional finite element software package, MAGNA/FIM. The electric lines of force have almost perpendicular incident angles to the alumina surface in this electrode configuration.

3 EXPERIMENTAL RESULTS

We observed the discharged light emission by surface flashover using a still camera. The observation result is shown in Figure 6. The surface flashover started at the high voltage electrode and developed straight forward to the ground electrode.

Figure 7 shows the influence of the surface charging potential on the surface flashover voltage. When the surface charges were located at the starting point of surface discharge (Case A), a positive charge reduced the negative surface flashover voltage and a negative charge raised the negative surface flashover voltage. On the other hand, when surface charges were located at a point that was 25 mm from the high voltage electrode (Case D), both positive and negative charges reduced the negative surface flashover voltage.

In addition, the influence of negative charge on surface flashover voltage differs with the location of the negative charge, that is, a negative charge that is located near the starting point of surface discharge (Case A and B) raised the negative surface flashover voltage and a negative charge located on the discharge path (Case C and D) reduced the negative surface flashover voltage. From these results, we found that the negative charge on the alumina surface had different effects with different locations of surface charge.

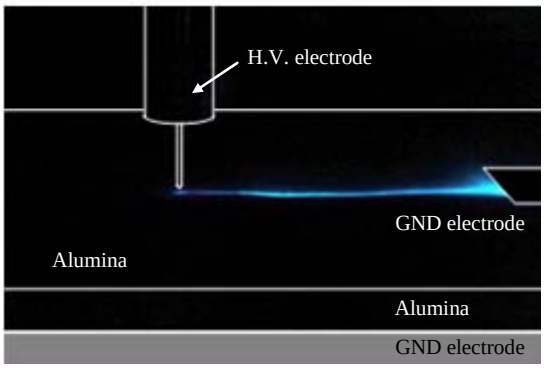

Figure 6. Discharge light emission by surface flashover.

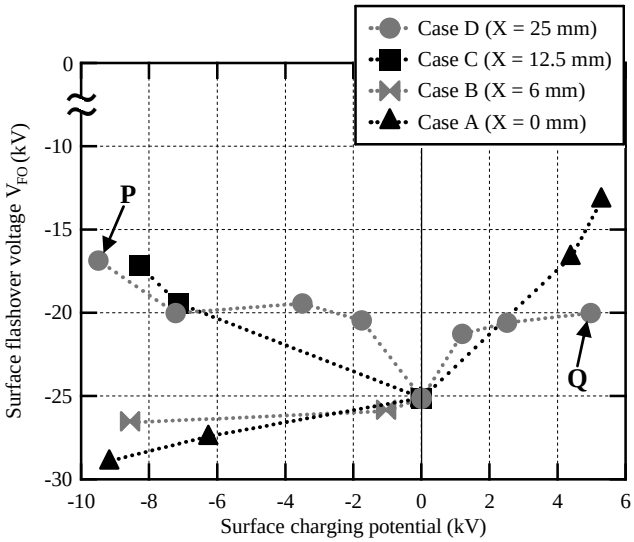

Figure 7. Influence of surface charging potential on surface flashover voltage. (applied dc voltage for charge, -25 kV to -35 kV or +25 kV to +35 kV)

4 DISCUSSIONS

4.1 INFLUENCE OF CHARGE ON SURFACE DISCHARGE INCEPTION

The surface charges of Case A may have a greater influence on surface discharge inception rather than the development of surface discharge. As for surface charges located near the cathode electrode, the electric field at the electron emission may be relaxed or enhanced by homo or hetero surface charges.

Figure 8 shows a relationship between surface charging potential of Case A and flashover electric field strength (E_p). E_p was defined as the electric field strength at 0.15 mm distance from the high voltage electrode. From Figure 8, E_p was 20-30 kV/mm, and independent of surface charging potential. Considering the surface roughness of the electrode, and that the field enhancement factor β is assumed to be about 10^2, the order of 10^7 V/m is appropriate. As a result, when the surface charge exists only near the cathode electrode, the surface discharge inception voltage is determined by the electric field strength at the point of electron emission.

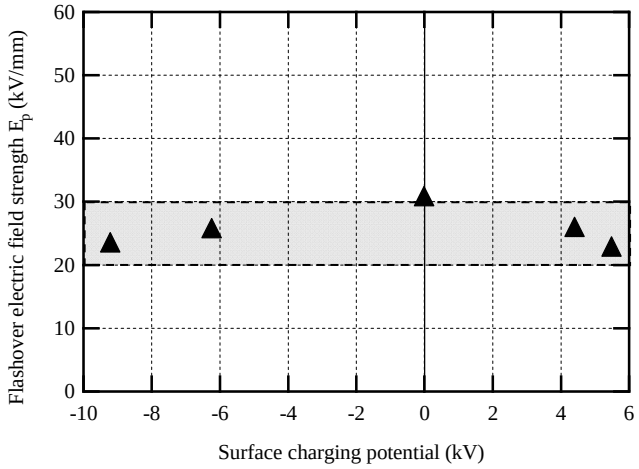

Figure 8. Relationship between surface charging potential and electric field strength. (Case A : X = 0 mm)

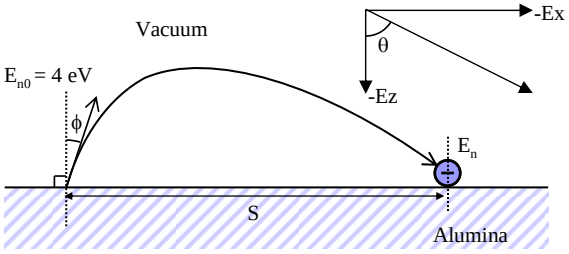

Figure 9. Schematic model of secondary electron trajectory.

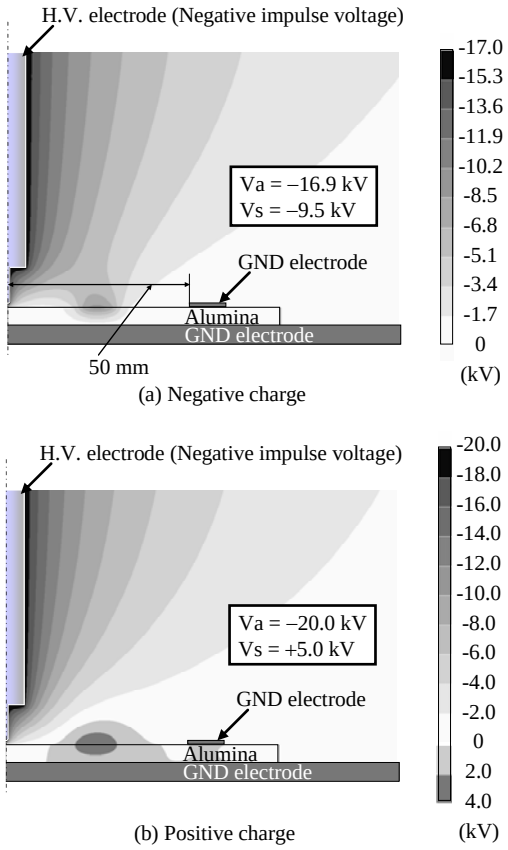

Figure 10. Equi-potential distribution with surface charge (Case D : X = 25 mm).

4.2 INFLUENCE OF CHARGE ON SURFACE DISCHARGE DEVELOPMENT

The surface charges of Case D may have a greater influence on the development of surface discharge rather than the discharge inception, because the surface charges may largely distort the electric field distribution on the alumina surface. As for the surface charge located on discharge path, the surface charge may change the conductive property of alumina dielectrics, secondary electron emission characteristics, and flight trajectory of secondary electrons.

In order to discuss the influence of surface charges on the flight of the secondary electron, we calculated the electric field along the alumina surface. From the result, we calculated the flight distance of a secondary electron and secondary electron energy at the collision against the alumina surface.

Figure 9 shows a schematic model of secondary electron trajectory. It is supposed that a secondary electron starts at an angle of ϕ with an initial energy of E_{n0}. The surrounding electric field vector at the starting point of the electron has the angle θ.

For our calculations, we assumed that the electric field is constant during the flight of the electron. We calculated the flight distance of secondary electron S and secondary electron energy E_n by the electron motion equation:

$$m\frac{d^2\vec{r}}{dt^2} = -e\vec{E} \qquad (1)$$

When solving equation (1) for X and Z directions and giving the initial conditions as described in Figure 9, we can obtain S from X at Z = 0 and E_n at the time of collision against the alumina surface from the velocity at Z = 0. Then, S and E_n are calculated as:

$$S = 2\frac{E_{n0}}{E_Z}\sin 2\phi\left(1+\frac{\tan\theta}{\tan\phi}\right) \qquad (2)$$

$$E_n = E_{n0}\left(1+4\sin\phi\cos\phi\tan\theta+4\cos^2\phi\tan^2\theta\right) \qquad (3)$$

Figure 10 shows calculation results of equi-potential distribution when surface charge exists on Case D. In order to compare the potential distribution and electric field distribution at flashover, we used the V_{FO} as the applied voltage in the calculation. Figure 10a shows the potential distribution for the negative charge (applied voltage Va = –16.9 kV, surface potential Vs = –9.5 kV which shows the case of point P in Figure 7), and Figure 10b shows the potential distribution for positive charge (applied voltage Va = –20.0 kV, surface potential Vs = +5.0 kV which shows the case of point Q in Figure 7).

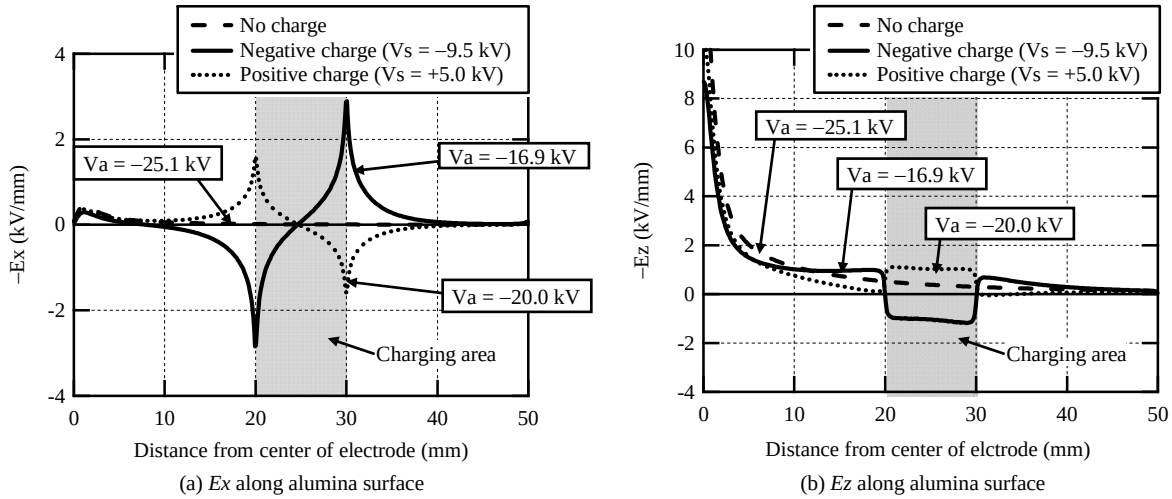

(a) *Ex* along alumina surface (b) *Ez* along alumina surface

Figure 11. Calculation result of electric field on the alumina surface.

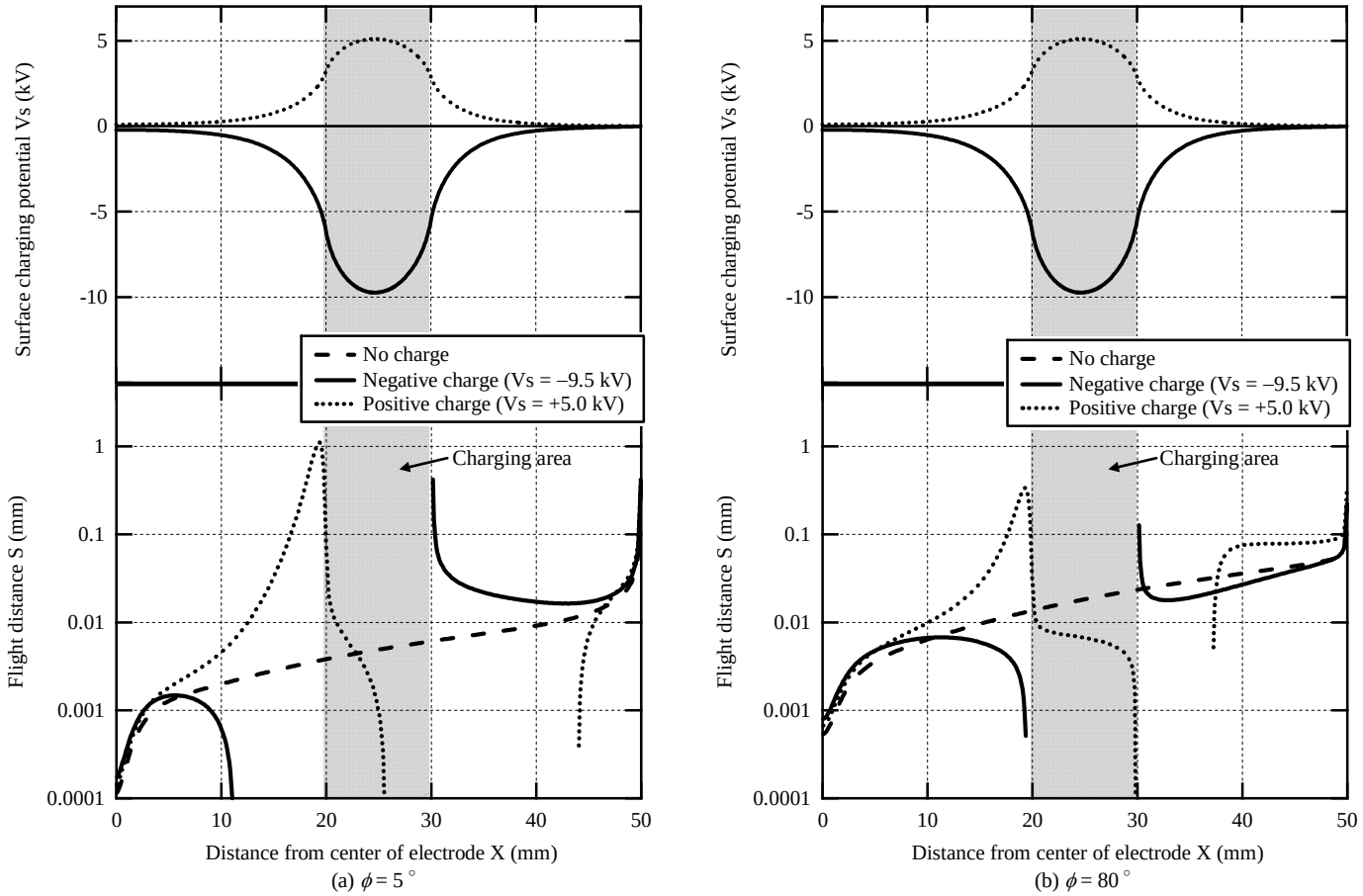

(a) $\phi = 5^\circ$ (b) $\phi = 80^\circ$

Figure 12. Flight distance of secondary electron.

Figure 11 shows the electric field around the alumina surface. Figure 11a shows the horizontal component of the electric field (*–Ex*) and Figure 11b shows the vertical component of the electric field (*–Ez*).

Figure 12 shows the flight distance of the secondary electron calculated in equation (2). When a negative charge exists, it becomes difficult for the secondary electron to fly in $X < 20$ and easy for it to fly in $30 < X$. When a positive charge exists, it becomes easy for the secondary electron to fly in $X < 20$ and difficult for it to fly in $30 < X$. In addition, when the secondary electron flies at an angle of $\phi = 5^\circ$, it is strongly influenced by surface charge more so than when a secondary electron flies at an angle of $\phi = 80^\circ$.

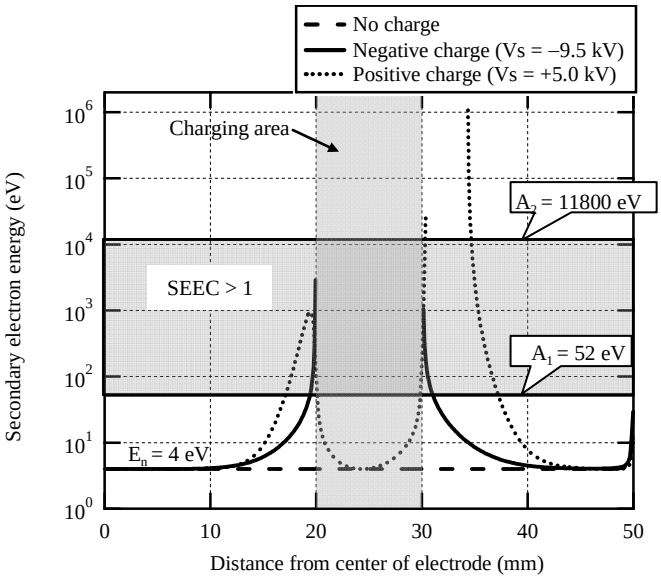

Figure 13. Secondary electron energy at collision against alumina surface.

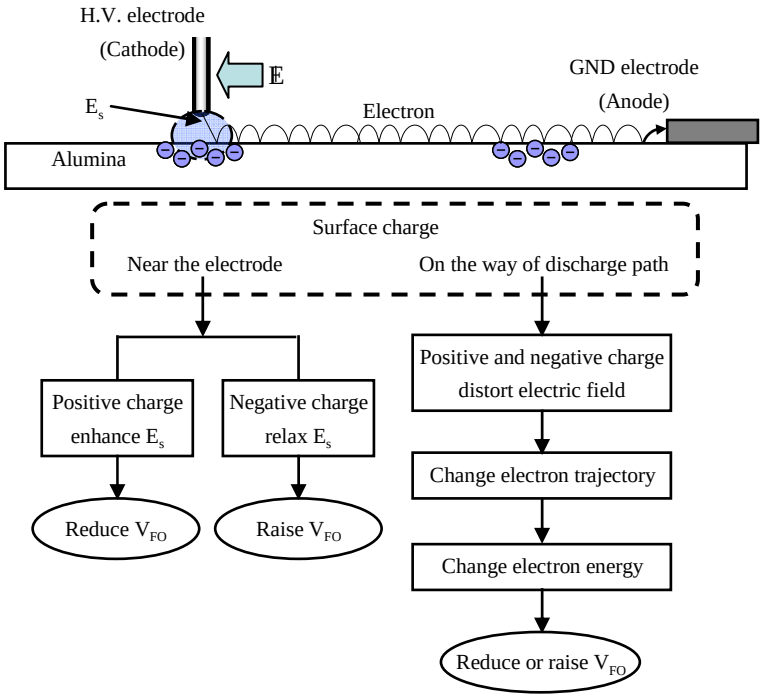

Figure 14. Mechanism of surface discharge influenced by surface charge.

Figure 13 shows secondary electron energy at the collision against the alumina surface in Equation (3) when a secondary electron flies at an angle of ϕ = 5 °. When no surface charge exists, E_n is 4 eV. In other words, E_n is the same as initial energy E_{n0}. The secondary electron emission coefficient (SEEC) of alumina is higher than 1 when the secondary electron energy is from 52 eV to 11800 eV [10]. So, when no surface charge exists, it is difficult for the secondary electron emission avalanche to appear. On the other hand, when surface charge exists, secondary electron energy is high enough to make the secondary electron emission avalanche.

As a result, the surface charge on the discharge path plays a role in making secondary electron energy high enough for the secondary electron emission avalanche. The mechanism of surface discharge influenced by surface charge can be illustrated in Figure 14. When surface charge is located near the electrode, a positive charge enhances the electric field at the end of the high voltage electrode E_s and therefore reduces the negative surface flashover voltage V_{FO}, and the negative charge relaxes E_s and therefore raises V_{FO}. When surface charge is located on the discharge path, both positive and negative charges distort the electric field, change electron energy and therefore reduce or raise V_{FO}.

5 CONCLUSIONS

We investigated the influence of surface charge on surface flashover characteristics in vacuum. The experimental results revealed that surface charge is a critical factor in the surface flashover phenomena. It was also clarified that the surface charge influences the inception and development of surface flashover characteristics. The experimental results were as follows:

(1) When surface charges were located near the cathode electrode, a positive charge made the surface flashover voltage lower and a negative charge made the surface flashover voltage higher.

(2) We could explain the results by the change in the electric field close to the cathode electrode at flashover.

(3) When surface charges were located at the discharge path, either positive or negative charges made the surface flashover voltage lower in our experiment.

(4) We could explain the results by the role of surface charge for making the secondary electron energy higher for satisfying the condition of secondary electron emission avalanche (SEEA).

REFERENCES

[1] J. Ballat, D. Konig and U. Reinighaus, “Spark conditioning procedures for vacuum interrupters in circuit breakers”, IEEE Trans. Electr. Insul., Vol. 28, pp.621-627, 1993.

[2] H. C. Miller, “Surface Flashover of Insulators”, IEEE Trans. Electr. Insul., Vol. 24, pp.765-786, 1989.

[3] H. C. Miller, “Flashover of Insulators in Vacuum”, IEEE Trans. Electr. Insul., Vol. 28, pp.512-527, 1993.

[4] R. V. Latham, *High Voltage Vacuum Insulation: Basic Concepts and Technological Practice*, Academic Press, 1995.

[5] O. Yamamoto, T. Takuma, M. Fukuda, S. Nagata, T. Sonoda, “Improving withstand voltage by roughening the surface of an insulating spacer used in vacuum”, IEEE Trans. Dielectr. Electr. Insul., Vol. 10, pp.550-556, 2003.

[6] Y. Tsukamoto, Y. Yamano, S. Kobayashi and Y. Saito, “Effect of in situ heat treatment on surface flashover characteristic and surface condition of alumina in vacuum”, 21st Intern. Sympos. Discharges Electr. Insul. Vacuum, pp. 118-121, 2004.

[7] H. Okubo, S. Yanabu, “Feasibility Study on Application of High Voltage and High Power Vacuum Circuit Breaker”, 20th Intern. Sympos. Discharges Electr. Insul. Vacuum, pp. 275-278, 2002.
[8] Y. Yamano, S. Ito, K. Kato, H. Okubo, Y. Hakamata, “Charging Characteristics and Electric Field Distribution on Alumina as Affected by Triple Junction in Vacuum”, IEEE Trans. Dielectr. Electr. Insul., Vol. 10, pp. 563-568, 2003.
[9] T. Hosono, K. Kato, A. Morita, H. Okubo, “Surface Charges on Alumina in Vacuum with Varying Surface Roughness and Electric Field Distribution”, IEEE Trans. Dielectr. Electr. Insul., Vol. 13, pp. 627-633, 2007.
[10] P. H. Dauson, “Secondary Electron Emission Yields of some Ceramics”, J. Appl. Phys., Vol. 37, pp. 3644-3645, 1964.

Katsumi Kato (M’09) was born on 20 May 1969. He received the Ph.D. degree in 1997 in electrical engineering from Nagoya University. Since 1997, he has been on the faculty of Nagoya University. Presently, he is an Assistant Professor of Nagoya University at the Department of Electrical Engineering and Computer Science. He is a member of IEE of Japan and IEJ.

Hidenori Kato was born on 17 January 1985. He received the B.S. degree in electrical engineering in 2007 from Nagoya University. Currently, he is a Master Course student of Nagoya University at the Department of Electrical Engineering and Computer Science.

Tsugunari Ishida was born on 14 July 1986. He received the B.S. degree in electrical engineering in 2009 from Nagoya University. Currently, he is a Master Course student of Nagoya University at the Department of Electrical Engineering and Computer Science.

Kenji Tsuchiya was born in Fukushima, Japan, on 1 April 1957. He received his bachelor degree in electrical engineering in 1981 from Waseda University, Japan. He joined Power & Industrial Systems Switchgear Design Department, Hitachi Ltd. in 2001, where he has been engaged in the development of medium-voltage switchgear and vacuum circuit breakers. He is a member of IEEJ

Hitoshi Okubo (M’81) was born on 29 October 1948. He received the Ph.D. degree in 1984 in electrical engineering from Nagoya University. He joined Toshiba Corporation, Japan in 1973 and was a manager of high voltage laboratory of Toshiba. From 1976 to 1978, he was at the RWTH Aachen, Germany and the TU Munich, Germany. In 1989, he was an Associate Professor and presently he is a Professor of Nagoya University at the Department of Electrical Engineering. He is a member of IEE of Japan, VDE and CIGRE.